

Fitting functions for a disk-galaxy model with different Λ CDM-halo profiles (Research Note)

L. Darriba and J.M. Solanes

Departament d'Astronomia i Meteorologia and Institut de Ciències del Cosmos, Universitat de Barcelona. C/ Martí i Franquès, 1;
E-08028 Barcelona, Spain
e-mail: ldarriba@am.ub.es, jm.solanes@ub.edu

Accepted: 7 April 2010

ABSTRACT

Aims. We present an adaptation of the standard scenario of disk-galaxy formation to the concordant Λ CDM cosmology aimed to derive analytical expressions for the scale length and rotation speed of present-day disks that form within four different, cosmologically motivated protogalactic dark matter halo-density profiles.

Methods. We invoke a standard galaxy-formation model that includes virial equilibrium of spherical dark halos, specific angular momentum conservation during gas cooling, and adiabatic halo response to the gas inflow. The mean mass-fraction and mass-to-light ratio of the central stellar disk are treated as free parameters whose values are tuned to match the zero points of the observed size-luminosity and circular speed-luminosity relations of galaxies.

Results. We supply analytical formulas for the characteristic size and rotation speed of disks built inside Einasto $r^{1/6}$, Hernquist, Burkert, and Navarro-Frenk-White dark matter halos. These expressions match simultaneously the observed zero points and slopes of the different correlations that can be built in the *RVL* space of disk galaxies from plausible values of the galaxy- and star-formation efficiencies.

Key words. dark matter – Galaxies: formation – Galaxies: fundamental parameters – Galaxies: spiral – Galaxies: structure

1. Introduction

In the current hierarchical galaxy-formation paradigm disk-galaxies are born out of the hot gas-atmospheres associated with the potential well of virialized cold dark matter (CDM) halos. It is assumed that baryons have initially both the same density profile and specific angular momentum distribution as DM – the latter achieved, for instance, through tidal interactions with neighboring objects in the precollapse phase (e.g. Peebles, 1969). As the gas radiates its energy it cools and starts to fall towards the center of the DM halo maintaining its specific angular momentum, where it settles into a rotationally supported disk. The assembly of a concentration of cold baryons at the bottom of the gravitational potential well on timescales longer than the free-fall time produces the adiabatic contraction of the dark halo¹. In this standard picture, the internal properties of disk galaxies are expected to be largely dictated by those of their host halos, and through the latter, by those of the background cosmology too.

Theoretical predictions for the distribution of disk galaxies in the space of disk scalelength (or size), fiducial (usually, maximum or asymptotic) rotational speed, and luminosity (or mass) based, partially or totally, on the scenario just outlined are abundant in the literature (e.g., Mo et al. 1998, hereafter MMW; Pizagno et al. 2005; Dutton et al. 2007). They are widely used in semi-analytic cosmological models, pre-prepared numerical

simulations of galaxy groups and clusters, and studies of disk-galaxy scaling relations.

While nowadays there are extensive and comprehensive investigations of the correlations between disk-galaxy properties that deal with the scatter and covariances of the variables and allow for different modes of halo contraction (e.g. Dutton et al., 2007), it is not always feasible to implement such sophisticated treatments whenever one needs to estimate the scaling of the basic structural and kinematic parameters of galaxies. The simplest alternative is the use of scaling laws derived directly from fits to a given set of observations. However, because of their lack of theoretical foundation, these formulas cannot be extrapolated to explain the properties of galaxies other than those from which they are derived. Halfway between these two options is the possibility of using analytical expressions endowed with a physical basis that enables their application to a wide range of galactic and halo parameters. It is precisely with this aim that we here introduce a self-consistent pure disk-formation model that follows the well-known approach by MMW adapted to the canonical Λ CDM concordance cosmology and to four different mass-density distributions for the protogalactic dark halos. This updated scenario is capable of matching *simultaneously* with very good accuracy the zero points and slopes of the observed correlations in the *RVL* space of disk galaxies from reasonably realistic values of its input parameters. Yet its most valuable characteristic is its ease of implementation, as we approximated the model predictions for the scale length and rotation speed of disks by analytical expressions. The supplied equations can come in handy for situations that require the generation of large numbers of galaxies with intrinsic attributes in good agreement with the

¹ In modern literature, the mode and amount of halo contraction are actually a matter of debate (e.g. Dutton et al., 2007; Tissera et al., 2009). The outcome, however, remains unchanged: the properties of disk galaxies are linked to those of their host halos.

mean observed trends, especially when the relative abundances of these objects are known in advance.

2. Model components

We recap here the key assumptions and associated equations of our self-consistent Λ CDM-model of disk-galaxy formation:

1. *In the protogalactic state, the (hot) baryons and dark matter are well mixed within virialized spherical halos. Both components have the same distribution of specific angular momentum.*

The total angular momentum J_{vir} of a galactic halo of virial mass M_{vir} is commonly characterized in terms of the dimensionless spin parameter

$$\lambda = \frac{J_{\text{vir}}/M_{\text{vir}}}{\sqrt{2}R_{\text{vir}}V_{\text{vir}}} f_c^{1/2}, \quad (1)$$

which, according to the results of N -body simulations, follows a lognormal distribution with median λ_0 lying in the range $0.03 \lesssim \lambda_0 \lesssim 0.05$ (see, for instance, Shaw et al. 2006 and references therein), nearly independent of cosmology, halo environment, and redshift (e.g. Lemson & Kauffmann, 1999). In Eq. (1), R_{vir} is the virial radius inside which the halo mean density, $\bar{\rho}_{\text{vir}}$, is Δ_{vir} times the mean density of the universe at the redshift of observation, $V_{\text{vir}}^2 = GM_{\text{vir}}/R_{\text{vir}}$, and f_c is a dimensionless function of the halo concentration (see below) that measures the deviation of the protogalactic halo's energy from that of a singular isothermal sphere with the same mass, $-(1/2)M_{\text{vir}}V_{\text{vir}}^2$ (see MMW). For the family of flat ($\Omega_m + \Omega_\Lambda = 1$) cosmologies, $\Delta_{\text{vir}}(z) \approx \{18\pi^2 + 82[\Omega(z) - 1] - 39[\Omega(z) - 1]^2\}/\Omega(z)$ (Bryan & Norman, 1998).

The halo concentration parameter, c , characterizes the overall shape of a halo density profile by measuring the ratio between its outer radius and inner scalelength. Originally introduced for the Navarro-Frenk-White function, its mean values are strongly correlated with the halo mass given a cosmology (e.g. Navarro et al., 1997). We approximate the mean concentration-mass relation at $z = 0$ in the range of halo masses of interest, $10^{10} \lesssim M/(h^{-1} M_\odot) \lesssim 10^{13}$, by the best-fitting power-law relation recently inferred by Macciò et al. (2008) from relaxed halos simulated in the Wilkinson Microwave Anisotropy Probe 5 years results (WMAP5) cosmology

$$c(M_{\text{vir}}, 0) = 9.35 \left[\frac{M_{\text{vir}}}{10^{12} h^{-1} M_\odot} \right]^{-0.094}, \quad (2)$$

where $c \equiv R_{\text{vir}}/r_{-2}$ is defined here in a profile-independent form by adopting as the inner characteristic radius of the halo density profile the radius r_{-2} , at which its effective logarithmic density slope $\gamma \equiv d \ln \rho(r)/d \ln r$ equals -2 . The WMAP5 cosmological parameters are $(\Omega_0, \Omega_{\Lambda,0}, \Omega_{b,0}, h, \sigma_8, n) = (0.26, 0.74, 0.044, 0.72, 0.8, 0.96)$, implying that $\bar{\rho}_{\text{vir}} \sim 96$ times the critical density for closure at the current epoch.

2. *Disks form smoothly out of cooling flows preserving the specific angular momentum of the baryons. The cold gas settles in centrifugal equilibrium at the center of the halo's potential well following an exponential distribution.*

The fraction of baryons that collect into the central galaxy (in the form of stars + cold gas) is defined as

$$m_d = M_d/M_{\text{vir}}, \quad (3)$$

where the values of this parameter, for which a plausible upper limit is the universal baryon fraction $f_{b,0} = \Omega_{b,0}/\Omega_0 \approx 0.17$, do not seem to depend much on the halo mass or spin (Sales et al., 2009). Similarly, the angular momentum of the disk, expressed in units of that of its surrounding halo, can be written as

$$j_d = J_d/J_{\text{vir}}. \quad (4)$$

The common yet uncertain assumption that the specific angular momenta of the central disk galaxy and of the halo hosting it are equal, $J_d/M_d = J_{\text{vir}}/M_{\text{vir}}$, is equivalent to setting $j_d = m_d$.

On the other hand, a thin exponential mass distribution of total mass M_d , surface density $\Sigma(R) = M_d/(2\pi R_d^2) \exp(-R/R_d)$, and a rotation curve $V(R)$, has a total angular momentum

$$J_d = 2M_d R_d V_{\text{vir}} \frac{1}{2} \int_0^\infty u^2 e^{-u} \frac{V(uR_d)}{V_{\text{vir}}} du \equiv 2M_d R_d V_{\text{vir}} f_{Rd}^{-1}, \quad (5)$$

where the factor f_{Rd} is unity for a disk with a flat rotation curve at the level V_{vir} , and where the total circular speed is computed by summing in quadrature the contributions from the disk of cold baryons, V_d , and from the dark halo, V_h ,

$$V^2(R) = V_d^2(R) + V_h^2(r=R), \quad (6)$$

with R the cylindrical radius. An expression for $V_d^2(R)$ can be found in Binney & Tremaine (2008), p.101, Eq. (2.165).

Substituting Eqs. (1), (3), and (4) into Eq. (5), one can then obtain the disk scalelength as a function of the model parameters

$$R_d = \frac{f_{Rd}}{\sqrt{2}f_c} \lambda_d R_{\text{vir}}, \quad (7)$$

with $\lambda_d \equiv (j_d/m_d)\lambda$ the effective spin of the disk.

3. *The halo contracts adiabatically and without shell crossing to gas inflow.*

According to the adiabatic compression paradigm (Blumenthal et al., 1986), for a spherical halo in which all particles move on circular orbits with velocity $V(r)$, any function of the specific angular momentum $rV(r)$ is an adiabatic invariant. Assuming that the initial and final mass distributions of the different components are spherically symmetric, this invariance leads to the relationship

$$[M_d(r) + M_i(r_i)(1 - m_d)]r = M_i(r_i)r_i, \quad (8)$$

where r_i and r are, respectively, the initial and final radius of the spherical shells, $M_i(r)$ is the initial protogalactic halo mass profile, and $M_d(r)$ comes from the replacement of the final thin exponential disk configuration by the spherical density profile that has the same enclosed mass.

The contribution to the total rotation curve (Eq. [6]) from the dark matter (and the remaining hot baryons) is therefore

$$V_h^2(r) = GM_i(r_i)(1 - m_d)/r. \quad (9)$$

Taking into account that both halo and disk properties are directly proportional to their corresponding virial parameters, Eq. (6) allows one to express the amplitude of the total rotation curve at a given number of scalelengths and, in particular, its peak value, V_{max} , in the compact form (cf. MMW)

$$V_{\text{max}} = V_{\text{vir}} f_{v\text{max}}, \quad (10)$$

with $f_{v\text{max}}$ a dimensionless factor that, like f_{Rd} , depends on the adopted halo density law and on the values of parameters λ_d , c , and m_d .

Table 1. Halo profiles.

Profile	$\tilde{\rho}(s)$	c/c_s	Reference
EIN ₆	$\exp(1 - s^{1/6})$	12^{-6}	Einasto & Haud (1989)
HER	$8/s/(1 + s)^3$	2	Hernquist (1990)
BUR	$4/(1 + s)/(1 + s^2)$	0.6573	Burkert (1995)
NFW	$4/s/(1 + s)^2$	1	Navarro et al. (1997)

3. Model predictions

We now proceed to tune the free parameters of our disk-galaxy formation model to match the scaling relations in *RVL* space observed at $z \sim 0$. For a given halo virial mass, two are the free parameters in our modeling: the disk mass fraction, m_d , and mass-to-light ratio, $\Upsilon_d \equiv M_d/L$. This latter quantity is needed to convert the predicted disk masses into observed luminosities. We do not allow the average effective disk spin to vary freely however, but use the condition $j_d = m_d$ to set it equal to three representative values of λ_0 : 0.03, 0.04, and 0.05².

We investigated the performance of our model for the four functional forms of protogalactic DM halos listed in Table 1. They are among the most representative functions used in the literature to describe the equilibrium density profiles of halos generated in CDM N -body simulations. All of them are spherical density distributions of the form

$$\rho(r) = \rho_s \tilde{\rho}(s), \quad (11)$$

where $\rho_s \equiv \rho(r_s)$ and r_s are the characteristic density and scale radius of the profile respectively, and $\tilde{\rho}(s)$ is a dimensionless function of the dimensionless radius $s \equiv r/r_s$.

With the aid of the $c(M_{\text{vir}})$ relation these expressions can be reduced to uniparametric³ density laws in which the halo structure is fully determined from M_{vir} . It can be shown that

$$\rho_s = \frac{1}{3} \bar{\rho}_{\text{vir}} c_s^3 \int_0^{c_s} s^2 \tilde{\rho}(s) ds, \quad (12)$$

where the characteristic concentration $c_s \equiv R_{\text{vir}}/r_s$ is directly related to the profile-independent halo concentration parameter c defined in Eq. (2) (see Table 1).

In order to constrain our model predictions, we consider a subset of the SFI++ sample (Springob et al., 2007) consisting of 649 galaxies also included in the compilation of ~ 1300 local field and cluster spiral galaxies by Courteau et al. (2007). The full SFI++ contains measures of intrinsic rotation velocity widths reduced to a homogeneous system based on the 21 cm spectral line, W , as well as absolute I -band magnitudes for near 5000 spiral galaxies, while the dataset by Courteau et al. provides inclination-corrected estimates of disk scalelengths also in the I -band (below both observables and model parameters will refer to this near-IR band).

As stated by Catinella et al. (2007), for most intermediate and bright disks the width of the global HI profile provides a more reliable observational estimate of the peak rotation velocity than the widths of H α rotation curves, at least for objects not affected by environmental interactions. This is probably because the latter are usually evaluated either at a radius where,

² We ignore here a possible dependence of this parameter on halo mass (e.g. Berta et al., 2008).

³ The Einasto $r^{1/n}$ model has an additional parameter n controlling the curvature of the profile. In our modeling this parameter is kept fixed to $n = 6$, a value representative of galaxy-sized halos (Merrit et al., 2005).

Table 2. Model parameters.

Profile	λ_d	m_d	$\Upsilon_d/[h(M/L)_\odot]$	$V_{\text{max}}/V_{\text{vir}}$
EIN ₆	0.03	0.025	1.20	1.4
EIN ₆	0.04	0.050	1.50	1.6
EIN ₆	0.05	0.080	1.70	1.8
HER	0.03	0.020	1.00	1.4
HER	0.04	0.035	1.25	1.5
HER	0.05	0.055	1.45	1.7
BUR	0.03	0.030	1.50	1.4
BUR	0.04	0.050	1.60	1.6
BUR	0.05	0.075	1.75	1.7
NFW	0.03	0.030	1.30	1.4
NFW	0.04	0.050	1.50	1.6
NFW	0.05	0.080	1.70	1.8

on average, they are still rising (e.g., $2.2R_d$), or on the asymptotic part of the optical disk. Accordingly, we adopt the approximation $W/2 \simeq V_{\text{max}}$, where V_{max} is the maximum width of our model total speed curve measured within $5R_d$.

3.1. Scaling laws

The distribution of R as a function of V provides the most effective way of determining the value of m_d – which for bright galaxies represents to a good approximation the stellar mass fraction – that best fits the observations for each one of the values of λ_d under consideration. To allow for a more robust comparison between the model predictions and the data, the *RV* scaling law has been recast in the form of the tighter relation between the average specific angular momentum of disks computed from the fiducial rotation speed of the galaxies, $\iota_d = 2R_d V_{\text{max}}$, and V_{max} . In a log-log scale this relationship is expected to follow a straight line with a slope near 2 and a zero point that is a sensitive function of m_d .

In the upper-left panel of Fig. 1, we show the model relations that best fit the barycenter of the data cloud for the four halo profiles considered and the central value of λ_d (the best values of m_d obtained for each one of the three values adopted for λ_d are listed in Col. 3 of Table 2). It can be seen from this plot that our disk models also reproduce the slope of the observed $\iota_d - V_{\text{max}}$ scaling law. We note in passing that on the basis of its location in this diagram, the angular momentum and disk scale of the Milky Way (MW) are unrepresentative of those of a typical spiral (see also Hammer et al., 2007).

With m_d fixed and given that the halo concentration is not allowed to vary freely, the most sensitive tuning of the other free parameter of the model, Υ_d , is achieved by normalizing the model predictions to the observed VL relation. For the latter, which is fully independent of surface brightness (Zwaan et al., 1995; Courteau & Rix, 1999), we use the calibration of the Tully-Fisher (TF) relationship corrected from observational and sample biases calculated by Masters et al. (2006) using 807 cluster galaxies extracted from the SFI++ catalog, which we rewrite in the form

$$M_I - 5 \log h = -20.85 - 7.85 [\log(2V_{\text{max}}) - 2.5] \quad (13)$$

to facilitate the comparison with our model predictions. In Eq. (13), $M_{I,\odot} = 4.11$ mag has been adopted to transform model luminosities into absolute magnitudes. As in the former case, the upper-right panel of Fig. 1 shows that the predicted VL relations (again we show only those inferred using the central value of λ_d) closely match the slope of the empirical estimate. In this case,

the best values of Υ_d have been set by minimizing the residual between the model predictions and the observed TF relationship over the full available range of velocities. As could be expected, the agreement between the model predictions and our SFI++-based comparison sample is fairly good too. This panel also illustrates the well-known deficiency in luminosity of the MW with respect to the TF relation (Portinari et al., 2007).

The excellent agreement between predictions and observations in the *RV* and *VL* planes is maintained for the joint distribution of the three variables. The lower-left panel of Fig. 1 depicts, again for the central value of λ_d , the scatter diagram of central disk surface density, $\Sigma_0 = M_d/(2\pi R_d^2)$, and rotation speed. We have converted Springob et al.’s data on M_J into total disk luminosities, which in turn have been transformed into disk masses using the values of Υ_d derived from the normalization of the *VL* relation. It can be seen that our model predictions are once more comfortably close to both the normalization and, in this case, *curved* mean trend delineated by the data.

3.2. Fitting functions for galaxy scaling parameters

By using the values quoted in Cols. 3 and 4 of Table 2 it is straightforward to calculate the average luminosity of a nearby disk embedded in a halo of given M_{vir} and λ_d . However, as shown in Sect. 2, each of the remaining fundamental disk properties, the characteristic scale and rotation speed, participates in the calculation of the other. As a result, they can only be computed by applying an iterative procedure that, despite its fast convergence, remains cumbersome. For this reason, it is very convenient to approximate the dimensionless factors f_{Rd} and $f_{V_{\text{max}}}$ appearing in the calculation of R_d and V_{max} (eqs. [7] and [10], respectively) by fitting functions. Drawing inspiration from MMW, we propose the following fitting formulas, which are valid for any of the protogalactic halo mass density profiles explored:

$$f_{Rd}(\lambda_d, c, m_d) \approx \left(\frac{\lambda_d}{0.05}\right)^{a_1+a_2m_d/(1+\lambda_d)} (a_3 + a_4m_d + a_5m_d^2) \times [a_6 + a_7c + a_8/c + a_9/(cm_d)], \quad (14)$$

$$f_{V_{\text{max}}}(\lambda_d, c, m_d) \approx \left(\frac{\lambda_d}{0.05}\right)^{0.001/m_d+b_1m_d} (b_2 + b_3m_d + b_4m_d^2) \times (b_5 + b_6c + b_7/c). \quad (15)$$

The values of the coefficients corresponding to each profile, which are independent of the adopted $c(M_{\text{vir}})$ relation, are listed in Table 3. Both approximations are accurate to within 8 % for $5 \leq c \leq 25$, $0.03 \leq \lambda_d \leq 0.05$, and $0.01 \leq m_d \leq 0.1$. We note that attempts to fit these dimensionless factors using either solely polynomials or a linear combination of power laws of parameters λ_d , c , and m_d have required a substantially larger number of terms to achieve a similarly satisfactory match. Given the countless number of real functions that can be implemented, it would be obviously possible to find other formulae also producing good fits, but most likely they will be more complicated than the above expressions.

4. Discussion and conclusions

We formulated a standard formation model of disk galaxies inside DM halos within the concordant Λ CDM cosmology that simultaneously predicts with high accuracy the main trends of the observed fundamental scaling relations of nearby galaxies in *RVL* space. This modeling has been developed with the sole

aim of deriving physically sound analytical expressions for predicting the central properties that characterize the light profiles and rotation curves of *typical spirals*. We supply formulas for Einasto $r^{1/6}$, Hernquist, Burkert, and Navarro-Frenk-White protogalactic halo mass density distributions that provide a similarly good overall description of the data on disks for realistic enough values of the model free parameters. We find that, for a given λ_d , the predictions of the Einasto $r^{1/6}$, Hernquist, and Navarro-Frenk-White profiles are relatively similar, while the Hernquist profile – the only density law investigated that does not follow a $\rho \propto r^{-3}$ behavior near R_{vir} – requires values of m_d and Υ_d that are lower by about a factor of 0.70 and 0.85, respectively.

The reader may have noticed that our best models yield for Υ_d , i.e. for the inverse of the average star-formation efficiency, values somewhat lower than those inferred from population synthesis calculations (e.g. Pizagno et al., 2005). We stress however that the observational estimates of this parameter are affected by considerable uncertainties, our prediction that the average mass-to-light ratio of disks is $\sim 1(M/L)_\odot$, which is consistent with submaximal disks arguments (Courteau & Rix, 1999; Kuzio de Naray et al., 2008), as well as relatively close to the values adopted as input in more sophisticated models of disk formation (Dutton et al., 2007). On the other hand, we find that the predicted values of m_d are directly correlated with those adopted for λ_d . In particular we note that a value of $\lambda_d = 0.03$, which coincides with the median of the distribution of the spin parameter for relaxed halos derived by Macciò et al. (2008), implies a small current average galaxy-formation efficiency, $m_d/f_{b,0} < 0.2$. This agrees well with the predictions of galaxy evolution from halo occupation models (Zheng et al., 2007) and methods that match the stellar mass function to that of the halo (Conroy & Wechsler, 2009). Further recent support for low m_d (and λ_d , according to our model) comes for instance from weak lensing measurements (Mandelbaum et al., 2006) and from the roughly universal distributions of this parameter obtained by Sales et al. (2009) for various implementations of feedback in large cosmological N -body/gasdynamical simulations. Notice also the fifth column in Table 2, where we list the ratio $V_{\text{max}}/V_{\text{vir}}$ calculated for a MW-mass halo, which increases with increasing λ_d and decreasing M_{vir} . As stated by Dutton et al. (2007), the relatively high values we predict for this ratio – a characteristic common to standard models – would likely hamper a simultaneous match to the galaxy LF that, according to semi-analytical models of galaxy formation, requires the condition $V_{\text{max}} \sim V_{\text{vir}}$.

We made no attempt to explore the scatter of the observed scaling relations and the covariance that exists between model parameters, except for Fig. 1, where we carry out a naive comparison between the spread of the data and that resulting from taking into account the predicted scale of the probability distribution of the halo concentration. Including this and other sources of scatter, such as the variance of the halo spin parameter, or the dependence of the concentration-mass relation on the adopted cosmology (e.g. Macciò et al., 2008), would undoubtedly enrich the analysis. Yet, a thorough investigation of scatter requires dealing with the joint probability distribution of all the parameters entering the model and, in particular, with all their covariances (not just the variances), which ideally should be corrected from measurement errors. This far exceeds the scope of our present research. We note in addition that efforts in the direction just outlined will soon be much more effective when they can be applied to objective, homogeneous, and complete *RVL* datasets free of nontrivial selection biases, as those build from the cross-correlation of wide-area spectroscopic optical and HI surveys (e.g., Toribio et al. 2010, in preparation).

Table 3. Coefficients of the approximations.

Profile	a_1	a_2	a_3	a_4	a_5	a_6	a_7	a_8	a_9
EIN ₆	-0.041	5.95	0.264	-1.45	3.35	3.16	-0.0311	5.58	-
HER	-0.037	4.86	0.252	-1.73	6.14	3.13	-0.0429	7.62	-
BUR	-0.058	5.50	0.275	-1.20	0.70	2.63	-0.0234	7.44	0.027
NFW	-0.056	6.18	0.267	-1.46	3.31	3.19	-0.0310	5.56	-
	b_1	b_2	b_3	b_4	b_5	b_6	b_7		
EIN ₆	-5.50	0.634	5.24	0.78	1.44	0.0343	-0.72		
HER	-5.58	0.792	6.78	0.16	1.35	0.0351	-1.77		
BUR	-4.24	0.722	4.91	2.24	1.32	0.0394	-1.03		
NFW	-5.38	0.651	5.38	0.84	1.41	0.0346	-0.82		

Finally, we wish to comment on the possibility of extending our model predictions to distant galaxies by adopting a $c(M_{\text{vir}})$ relationship of the form

$$c(M_{\text{vir}}, z) = c(M_{\text{vir}}, 0)g(z)^{-1}, \quad (16)$$

with $c(M_{\text{vir}}, 0)$ given in Eq. (2) and $g(z)$ the concentration growth factor, which can be taken proportional to $H(z)^{2/3}$, as found in a recent modification of the original Bullock et al. (2001) model for *WMAP* cosmologies by Macciò et al. (2008).

Acknowledgements. We thank the anonymous referee for his/her thorough review and appreciate the comments and suggestions, which significantly helped to improving the manuscript. This work is supported by the Spanish Dirección General de Investigación Científica y Técnica, under contract AYA2007-60366.

References

- Berta, Z. K., Jimenez, R., Heavens, A. F., & Panter, B. 2008, *MNRAS*, 391, 197
- Binney, J., & Tremaine, S. 2008, *Galactic Dynamics* (2nd. edition), Princeton University Press, Princeton, NJ
- Blumenthal, G. R., Faber, S. M., Flores, R., & Primack, J. R. 1986, *ApJ*, 301, 27
- Bryan, G. L., & Norman, M. L. 1998, *ApJ*, 495, 80
- Bullock, J. S., Kolatt, T. S., Sigad, Y., Somerville, R. S., Kravtsov, A. V., Klypin, A. A., Primack, J. R., & Dekel, A. 2001, *MNRAS*, 321, 559
- Burkert, A. 1995, *ApJ*, 447, L25 (BUR)
- Catinella, B., Haynes, M. P., & Giovanelli, R. 2007, *AJ*, 134, 334
- Conroy, C., & Wechsler, R. H. 2009, *ApJ*, 696, 620
- Courteau, S., Dutton, A. A., van den Bosch, F. C., MacArthur, L. A., Dekel, A., McIntosh, D. H., & Dale, D. A. 2007, *ApJ*, 671, 203
- Courteau, S., & Rix, H.-W. 1999, *ApJ*, 513, 561
- Dutton, A. A., van den Bosch, F., Dekel, A., & Courteau, S. 2007, *ApJ*, 654, 27
- Einasto, J., & Haud, U. 1989, *A&A*, 223, 89 (EIN)
- Hammer, F., Puech, M., Chemin, L., Flores, H., & Lehnert, M. D. 2007, *ApJ*, 662, 322
- Hernquist, L. 1990, *ApJ*, 356, 359 (HER)
- Kuzio de Naray, R., McGaugh, S. S., & de Blok, W. J. G. 2008, *ApJ*, 676, 920
- Lemson, G., & Kauffmann, G. 1999, *MNRAS*, 302, 111
- Macciò, A. V., Dutton, A. A., & van den Bosch, F. C. 2008, *MNRAS*, 391, 1940
- Mandelbaum, R., Seljak, U., Kauffmann, G., Hirata, C. M., & Brinkmann, J. 2006, *MNRAS*, 368, 715
- Masters, K. L., Springob, C. M., Haynes, M. P., & Giovanelli, R. 2006, *ApJ*, 653, 861
- Merrit, D., Navarro, J. F., Ludlow, A., & Jenkins, A. 2005, *ApJ*, 624, L85
- Mo, H. J., Mao, S., & White, D. M. 1998, *MNRAS*, 295, 319 (MMW)
- Navarro, J. F., Frenk, C. S., & White, S. D. M. 1997, *ApJ*, 490, 493 (NFW)
- Peebles, P. J. E. 1969, *ApJ*, 155, 393
- Pizagno, J., et al. 2005, *ApJ*, 633, 844
- Portinari, L., Holmberg, J., & Flynn, C. 2007, *The Milky Way and the Tully Fisher Relation*, in *Island Universes*, ed. R. S. de Jong, *Astrophysics and Space Science Proceedings* (Springer, Netherlands), 57
- Sales, L. V., Navarro, J. F., Schaye, J., Dalla Vecchia, C., Springel, V., Hass, M. R., & Helmi, A., 2009, *MNRAS*, 399, L64
- Shaw L. D., Weller J., Ostriker J. P., & Bode P. 2006, *ApJ*, 646, 815
- Springob, C. M., Masters, K. L., Haynes, M. P., Giovanelli, R., & Marinoni, C. 2007, *ApJS*, 172, 599
- Tissera, P. B.; White, S. D. M., Pedrosa, S., & Scannapieco, C. 2009, *MNRAS*, submitted (arXiv:0911.2316)
- Wechsler, R. H., Bullock, J. S., Primack, J. R., Kravtsov, A. V., & Dekel, A. 2002, *ApJ*, 568, 52
- Zwaan, M. A., van der Hulst, J. M., de Blok, W. J. G., & McGaugh, S. S. 1995, *MNRAS*, 273, L35
- Zheng, Z., Coil, A. L., & Zehavi, I. 2007, *ApJ*, 667, 760

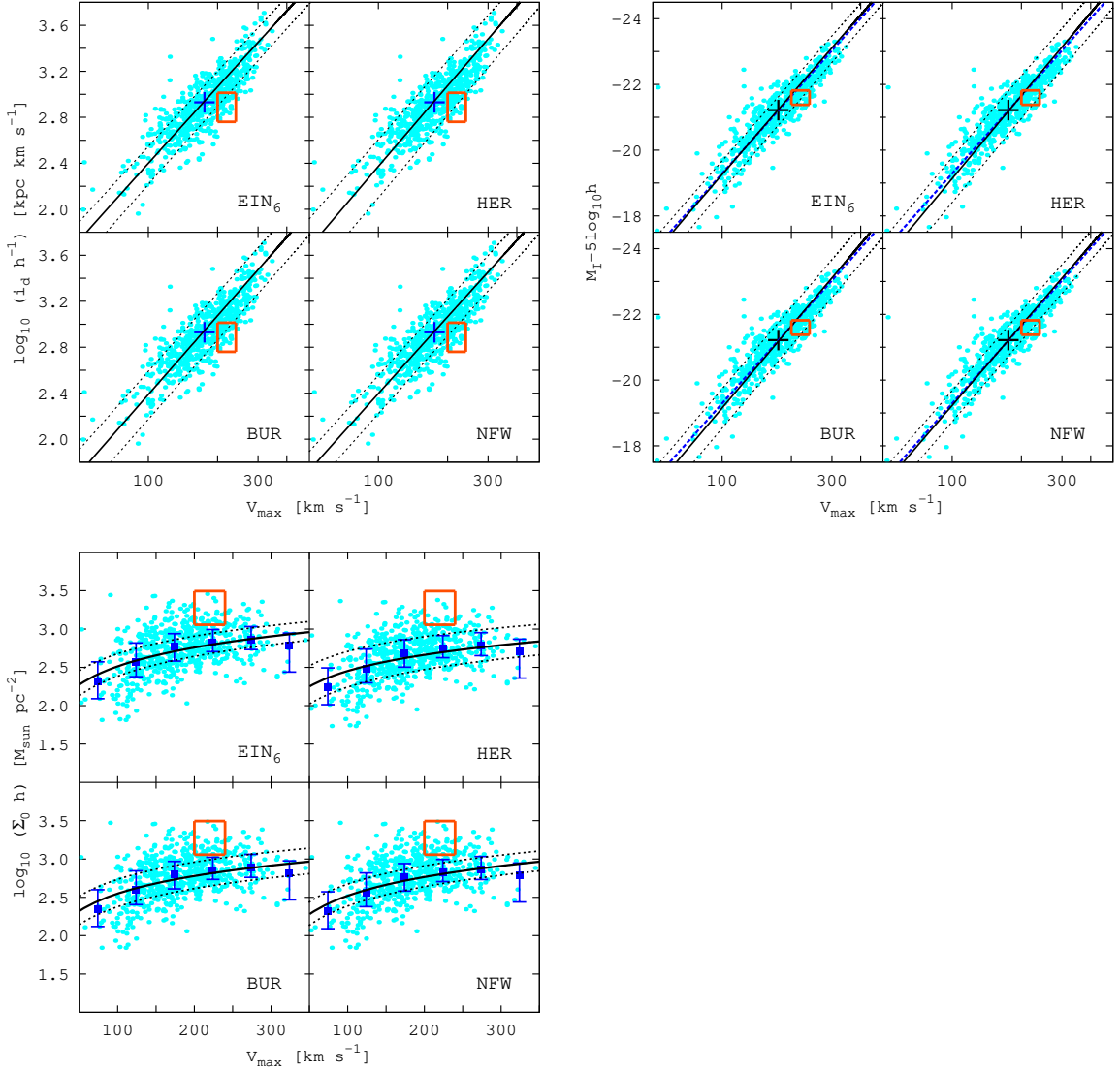


Fig. 1. Scale relations for nearby disks. *Upper-left:* Disk-specific angular momentum as a function of V_{\max} . The cross shows the barycenter of the data. *Upper-right:* I -band TF relation. The dashed line shows the one derived by Masters et al. (2006) from SFI++ data (Springob et al., 2007). The cross shows the barycenter of the data. *Lower-left:* Central-disk surface-mass density vs. V_{\max} . Squares with error bars show the median observational values and the first and third quartiles in each velocity bin. In all these plots the solid lines show model predictions for pure disks with $\lambda_d = 0.04$ using the mean $c(M_{\text{vir}})$ relation at $z = 0$, while the dotted curves show from top to bottom the predictions resulting from adopting the 2.3th and 97.7th percentiles of the concentration distribution (2σ scatter) assuming $\sigma_{\log c} = 0.11$ (Macciò et al., 2008). The error boxes represent, for comparison, the values measured for the MW from: $R_d = 2.5 \pm 0.5$ kpc, $M_d = 5 \pm 0.5 \times 10^{10} M_{\odot}$, and $V_{\max} = 220 \pm 20$ km s $^{-1}$ (Binney & Tremaine, 2008), and $L_I = (4 \pm 0.8) \times 10^{10} L_{\odot}$ (Portinari et al., 2007). The data clouds are build on the compilation of I -band absolute magnitudes and HI rotation widths by Springob et al. (2007) and on the I -band disk scalelength measurements by Courteau et al. (2007).